
ABSTRACT

The Venturimeter is a typical obstruction type flow meter, widely used in industries for flow measurement. The ISO standard (ISO-5167-1) provides the value of discharge coefficient for the classical machined Venturimeter in turbulent flows with Reynolds number above 2×10^5 at standard conditions. In the present work, an attempt is made to study and develop a computational model of a Venturimeter, which can be used as an efficient and easy means for predicting the compressibility effect using Computational Fluid Dynamics (CFD) software. ANSYS FLUENT-14 has been used as a tool to perform the modeling and simulation of flow through Venturimeter. Analysis of flow through Venturimeter has demonstrated the capability of the CFD methodology for predicting accurately the values of C_d , ϵ and C_{PL} over a wide range of operating conditions. CFD methodology also has been used to analyze the effect of various parameters like surface roughness, convergent and divergent angle as well as turbulent intensity of the incoming flow on the expansibility factor. It has been demonstrated that the validated CFD methodology can be used to predict the performance parameters of a classical Venturimeter even under conditions not covered by ISO 5167-1 standards.

KEYWORDS: Coefficient of Discharge, Computational Fluid Dynamics, Expansibility Factor, Venturimeter, Wall Roughness, Turbulent Intensity.

INTRODUCTION

The flow meters are being widely used in the industries to measure the volumetric flow rate of the fluids. These flow meters are usually differential pressure type, which measure the flow rate by introducing a constriction in the flow.

The pressure difference caused by the constriction is used to calculate the flow rate by using Bernoulli's theorem.

If any constriction is placed in a pipe carrying a fluid, there will be an increase in the velocity and hence the kinetic energy increases at the point of constriction. From the energy balance equation given by Bernoulli's theorem, there must be a corresponding reduction in the static pressure.

Thus by knowing the pressure differential, the density of the fluid, the area available for flow at the constriction and the discharge coefficient, the rate of discharge from the constriction can be calculated. The discharge coefficient (C_d) is the ratio of actual flow to the theoretical flow. The widely used flow meters in the industries are Orifice meter, Venturimeter and Flow Nozzle. Venturimeters and orifice meters are more convenient and frequently used for measuring flow in an enclosed ducts or channels.

Venturimeter are commonly used in single and multiphase flows. The objective of the present work is to study the compressibility effect on the Venturimeter parameters and to demonstrate the capability of the CFD methodology to predict accurately the values of C_d , ϵ and C_{PL} over a wide range of operating conditions. CFD methodology also has been used to analyze the effect of various parameters like surface roughness, convergent and divergent angle as well as turbulent intensity of the incoming flow on the effects of compressibility of fluids that are being meter.

The performances of these meters in terms of value of discharge coefficient and pressure loss have been investigated by several researchers. Gordon Stobie et al [1] made a performance study on effect erosion in a Venturi meter with

laminar and turbulent flow and low Reynolds number on discharge coefficient measurements. Diego A.Arias et al [2] conducted CFD analysis of compressible flow across complex geometry Venturi. Arun R et al [3] have predicted the values of discharge coefficient of Venturimeter at low Reynolds numbers by analytical and CFD method. Kenneth.C.Cornellus et al [4] have studied isentropic compressible flow for non ideal gas model for Venturi Nikhil Tamhankar at al [5] has investigated the Experimental and CFD analysis of flow through Venturimeter to determine the coefficient of discharge. It is observed from the above that the compressibility effect in the flow through Venturimeter has not been analyzed fully. Hence in the present study CFD has been used to study effect of compressibility effect of the fluid on the performance parameters of the Venturimeter over a wide range of operating conditions.

Principle of Venturimeter

The Venturimeter is an obstruction type flow meter named in honor of Giovanni Venturi (1746-1182), an Italian physicist who first tested conical expansion and contraction.

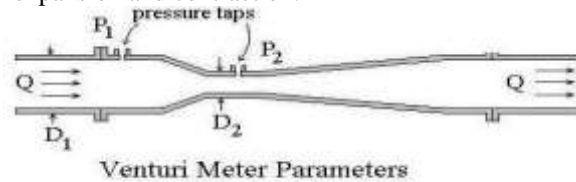


Fig.1: Classical Venturimeter

The classical Venturimeter consists of a converging section, throat and a diverging section as shown in the Fig.1. The function of the converging section is to increase the velocity of the fluid and temporarily reduce its static pressure. Thus the pressure difference between the inlet and the throat is developed. This pressure difference is correlated to the rate of flow of fluid by using Bernoulli's equation. As the theorem states that "In a steady, ideal flow of an incompressible fluid, the total energy at any point of fluid is constant, the total energy consists of pressure energy, kinetic energy and potential energy".

$$\frac{P_1}{\rho g} + \frac{V_1^2}{2g} + Z_1 = \frac{P_2}{\rho g} + \frac{V_2^2}{2g} + Z_1 \quad (1)$$

Because of the smoothness of the contraction and expansion section of venturi, the irreversible pressure loss is low. However, in order to obtain a significant measurable pressure drop, the downstream pressure tap is located at the throat of the Venturimeter. In comparison to the orifice meter, the pressure recovery is much better for Venturimeter. But there is no complete pressure recovery. Pressure recovery is measured as the pressure difference between inlet and outlet.

As per ISO 5167-1[7], the mass flow rate in a Venturimeter (Q_m in kg/s) for a compressible fluid is given by:

$$Q_m = \frac{\epsilon C_d}{\sqrt{1-\beta^4}} \frac{\pi d^2}{4} \sqrt{2\Delta P \rho_1} \quad (2)$$

Where: C_d is the discharge coefficient

β is the diameter ratio= d/D

d is the Venturimeter throat diameter, m

D is the upstream pipe diameter, m

ΔP is the differential pressure, Pa

ϵ is the expansibility factor

ρ_1 is the density at upstream pressure tap location, kg/m^3

Eqn.2 is based on the assumptions that the flow is steady, incompressible, and in viscid flow. However in order to take into account the real fluid effects like viscosity and compressibility, empirical coefficients C_d and ϵ are

introduced in the Eqn.2 In this paper we are analyzing the compressibility hence the empirical Coefficient ϵ is introduced in this analysis and for incompressible flow ϵ becomes unity.

Expansibility Factor or Expansion Factor (ϵ)

If the fluid is metered with compressible effect, the change in the density takes place as the pressure changes from p_1 to p_2 on passing through the throat section and it is assumed that there is no transfer of heat occurs, because of no work done by the fluid, and that expansion is isentropic.

The expansibility factor (ϵ) is calculated by using following empirical formula [ISO 5167 Standard].

$$\epsilon = \left[\left(\frac{K\tau^{2/K}}{K-1} \right) \left(\frac{1-\beta^4}{1-\beta^4\tau^{2/K}} \right) \left(\frac{1-\tau^{(K-1)/K}}{1-\tau} \right) \right]^{0.5} \quad (3)$$

The Eqn.3 is applicable only if $p_2/p_1 > 0.75$

The uncertainty of the expansibility factor is calculated by following correlation in terms of percent and is given by

$$\Delta\epsilon = ((4+100\beta^8) \Delta p/p_1) \% \quad (4)$$

CFD MODELING AND SIMULATION

CFD modeling is a useful tool to gain an additional insight into the physics of the flow and to understand the test results. The objective of the CFD work is to model the flow using 2D-axisymmetric Venturimeter geometry to study the flow characteristics that is similar to the practical situation.

The ANSYS FLUENT-14 CFD code is used to model and simulate the flow through Venturimeter. The Venturimeter geometry was modeled as a 2D-axisymmetric domain using unstructured grid. The dimensions of the geometry were taken from the ISO-5167-1 and no pressure taps were included in the CFD geometry.

The simulation was carried out for a standard classical Venturimeter with following dimensions (see Table. 1) and the model is shown in the Fig. 2

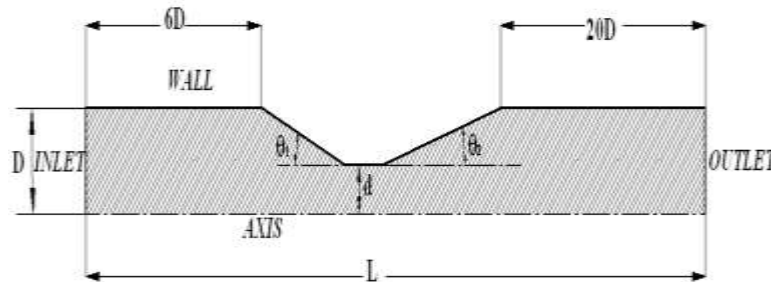


Figure 2 Classical Venturimeter

Table 1 :Dimensions of the Venturimeter Geometry

Variables	Values	Units
Diameter of pipe(D)	50	mm
Diameter of throat(d)	25	mm
Length of the throat	25	mm
Diameter Ratio(β)	0.5	---
Upstream pipe length	6D	mm
Downstream pipe length	20D	mm
Convergent angle(θ)	10	Deg
Divergent angle(ϕ)	7	Deg

Fig. 3 shows the CFD mesh used for the Venturimeter simulation. The geometry of the model includes 6D of straight pipe upstream of the convergent section and a 20D of straight pipe downstream of divergent section. The

convergent, throat and divergent region were meshed with very fine grids, while the upstream and downstream pipe region was meshed with coarser grids and boundary layer meshing was used near the wall.

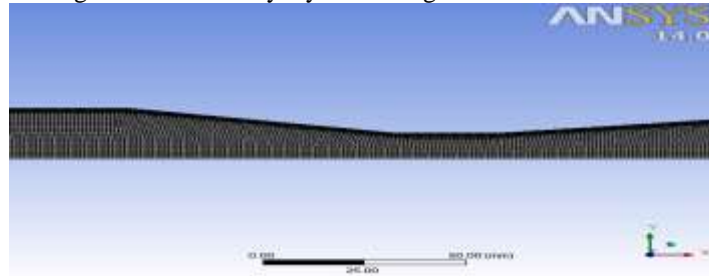


Figure 3 Mesh of Quadrilateral Elements Used For the Venturimeter for Analysis

VALIDATION OF CFD METHODOLOGY

For validation of CFD methodology a standard classical machined Venturimeter was selected. As per ISO-5167-1, the standard dimensions of a classical Venturimeter with a machined convergent section should be in the range,

$$50\text{mm} < D < 250\text{mm}$$

$$0.4 < \beta < 0.75$$

$$6 \times 10^5 < Re < 1 \times 10^6$$

Based on the standard limits, a Venturimeter with $D=50\text{mm}$ and $\beta=0.5$ was constructed as a 2D axis symmetric geometry. In the simulation procedure, the process of mesh generation is a very crucial step for better accuracy, stability and economy of prediction. Based on mesh convergence study, it is revealed that a total of quadrilateral elements beyond 120000 yields a consistent result. Hence a total of 155862 quadrilateral elements were used. In simulating a fully-developed flow through Venturimeter inlet, constant velocity was prescribed at the pipe inlet located $6D$ upstream of the upstream pressure tap. This will develop into a fully-developed turbulent velocity profile at the Venturi upstream pressure tap location.

The Realizable Spalart Allmars turbulence model with standard wall conditions was selected to model the flow domain. This choice was based on the computation made with different turbulence models (like K-omega standard, K-omega-SST and K-epsilon-standard) and the above model gives the best agreement for computed values of C_d with standard values.

For the validation, the fluid is selected is liquid with suitable boundary condition. Velocity at the inlet was specified as 3m/s and at outlet the gauge pressure was set to zero. The heat transfer from the wall of the domain was neglected. The solution was computed in the commercial CFD code FLUENT 14, in which the pressure based solver, was selected for this particular case. The computations were made at a Reynolds number of 6×10^5 and the computed value of C_d is 0.9895 which is within the uncertainty limits standard value given in ISO-5167 and hence CFD methodology was validated. The pressure and velocity contours along with velocity vectors are as shown in the Fig. 4. From the contours it is clearly observed that the velocity is increased in the convergent section with the corresponding reduction in the pressure, maximum velocity (minimum pressure) is recorded at the throat and velocity reduces in the divergent section while the pressure recovery occurs in this section. The vector plot shows the flow pattern of the fluid particles inside the Venturimeter.

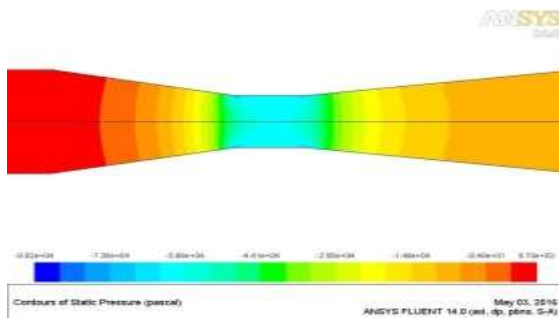


Figure 4(a) Pressure Contours

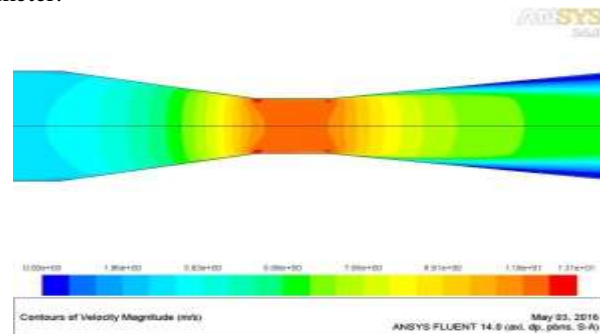


Figure 4(b) Velocity Contours

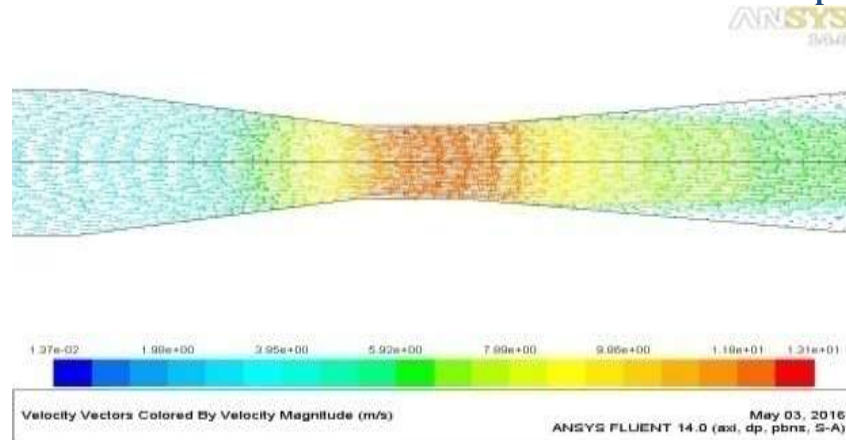


Figure 4(c) Velocity Vector

Figure 4 Pressure and Velocity Contours/ Vectors in the Venturimeter for Incompressible Flow ($D=50\text{mm}$, $\beta=0.5$, $Re=6 \times 10^5$)

RESULTS AND DISCUSSION

Having validated the CFD methodology, simulations were performed over a wide range of parameters. Venturimeter discharge coefficients were calculated from the CFD predicted venturi pressure drops. The simulations were done by keeping constant Reynolds number. Initially the simulation was carried out for a standard classical machined Venturimeter and the CFD results were validated with the standards. Further the studies were concentrated on compressibility effect, effect of wall roughness, by varying convergent and divergent angle, turbulent intensity and also permanent pressure loss are as follows:

A. Compressibility Effect on Venturimeter:

Computations are made for the Venturimeter ($D=50\text{mm}$, $\beta=0.5$ and $Re=6 \times 10^5$) for the flow of an incompressible fluid for different diameter ratios in the range 0.3 to 0.75. The results are tabulated in Table 2. Table 2 also shows the standard value of C_d as per ISO 5167. It is observed that the computed values of C_d are within the uncertainty limits of the standard values at all diameter ratios. It is also noted that the computed values are somewhat lower than the standard values.

This can be attributed to the fact that while modeling the geometry of the Venturimeter, the edges between convergent section and throat as well as upstream pipe are assumed to be sharp. However as per ISO 5167 a small fillet radius is to be given for these edges (ISO 5167). These sharp edges tend to increase the losses and hence results in somewhat lower values of C_d . Nevertheless, the values are within the permissible limits.

It is also seen that the computed value of C_d is independent of diameter ratio. Further the value is about 1% lower than theoretical value given in ISO 5167. But these deviations between the two sets of values of C_d are within the same order of magnitude as the uncertainty specified in the code. It is to be noted that the standard value of 0.995 given in ISO 5167 is valid for the diameter ratio in the range 0.4 to 0.75. However the computations have shown that even at $\beta=0.3$, $Re=6 \times 10^5$ agreement appears to be very good

Table 2 : Comparison between Computed and Standard Values of C_d for Incompressible Flow ($D=50\text{mm}$, $Re=6 \times 10^5$)

β	$C_d(\text{ISO})$	$C_d(\text{CFD})$	Deviation in %	$(C_d)_{\text{uncertainty in \%}}$
0.3	0.995	0.986	-0.89	± 1
0.4	0.995	0.985	-0.96	± 1
0.5	0.995	0.984	-1.0	± 1
0.6	0.995	0.983	-1.1	± 1
0.7	0.995	0.982	-1.2	± 1
0.75	0.995	0.981	-1.4	± 1

Computations have been made with air as working fluid to analyze the effect of compressibility. The air is assumed to be a perfect gas having a specific heat ratio of 1.4. Energy equations are also solved. Temperature at the inlet is 288K and the adiabatic boundary condition is specified at the outlet. Thus the CFD results give not only the variation in velocity and pressure but also the temperature and density variations are also computed. The boundary conditions specified for this analysis are constant inlet velocity with gauge pressure at outlet being zero. The computations have been made for different β ratio and constant Reynolds number 6×10^5 . For each run, the values of inlet velocity and viscosity are adjusted to obtain the desired Reynolds number. Further these parameters are chosen in a manner by which a wide range of $\Delta p/p_1$ is covered during the computation and the results are tabulated in the Table 3.

The comparison between the computed values of the Discharge coefficient and expansibility factor with the values given in ISO 5167 standard for the Venturimeter with pipe diameter is 50mm and $Re=6 \times 10^5$ is shown in Table 3. This Table also gives the codal values of the discharge coefficient for both incompressible and compressible flow. Further the values of $\Delta p/p_1$ are also tabulated. It is observed that the value of the discharge coefficient for compressible flow is always less than the incompressible flow. The ratio of the two represents the expansibility coefficient.

The value of ϵ calculated from the empirical correlation (ISO 5167 standard) is also given in the Table 3. The deviation in the computed values and ISO standard values of ϵ are observed to be of order of 1.25% in most of the cases. The range of $\Delta p/p_1$ covered in the analysis is from 0.26 to 0.08.

Table 3 : Comparison between the Computed and standard Values of C_d and ϵ for Venturimeter ($D=50\text{mm}$)

β	$\Delta p/p_1$	$(C_d)_{\text{Incom}}$	$(C_d)_{\text{com}}$	ϵ (CFD)	ϵ (ISO)
0.3	0.083	0.986	0.945	0.958	0.953
0.4	0.266	0.985	0.828	0.840	0.841
0.5	0.141	0.984	0.893	0.907	0.914
0.6	0.131	0.983	0.888	0.903	0.914
0.7	0.119	0.982	0.897	0.913	0.910
0.75	0.106	0.981	0.898	0.915	0.910

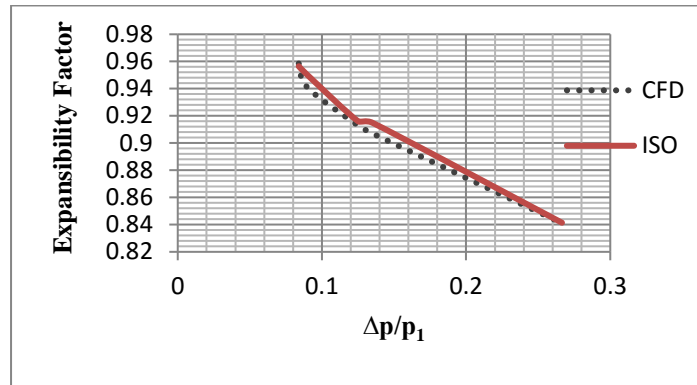


Figure 5 Variation of Expansibility Factor with Pressure Ratio ($D=50\text{mm}$, $Re=6 \times 10^5$, $\beta=0.3$ to 0.75)

Fig. 5 shows the variation of ϵ with $\Delta p/p_1$. It is seen that the agreement between computed and standard value of ϵ is excellent over the entire range of diameter ratios and $\Delta p/p_1$. Hence it is demonstrated that the validated CFD methodology can be used to predict the value of ϵ of a Venturimeter under varying conditions. It is interesting to note even for $\beta=0.3$, which is outside the limit specified by ISO 5167, the agreement is excellent. This gives the confidence that the CFD can be used to predict the compressibility effect in the Venturimeter even under non standard conditions. The contours of the velocity, pressure, density, temperature and velocity vectors for the flow through Venturimeter as shown in the Fig.6 for the compressible flows

The Fig. 6(a) shows the pressure contours. It is observed that the maximum pressure occurs when flow approaches in convergent region and pressure reduces when flow passes over the throat.

Fig. 6(b) shows the velocity contours. It is observed that the maximum jet velocity developed when fluid passes over the throat.

Fig. 6(c) shows the velocity vector plot. It is observed that the velocity maximum as jet comes out from the Venturimeter. Further a small separated flow region at end of divergent section where the flow is re-circulating is also clearly seen in the velocity vector plot.

Fig.6 (d) shows the density contours. It is observed that the density of the fluid decreases as it passes through the throat and then recovers as it flows through the divergent section. However the recovery is not complete and hence the density of fluid is lower at the outlet as compared to inlet. This can attributed the pressure drop in the Venturimeter.

Fig.6 (e) shows the temperature contours. It is observed that the temperature of the fluid decreases as it passes through the throat and then recovers as it flows through the divergent section, the average temperature at the outlet is 288.05K and inlet temperature is 288K. Hence the fluid heats up this can be attributed to viscous dissipation.

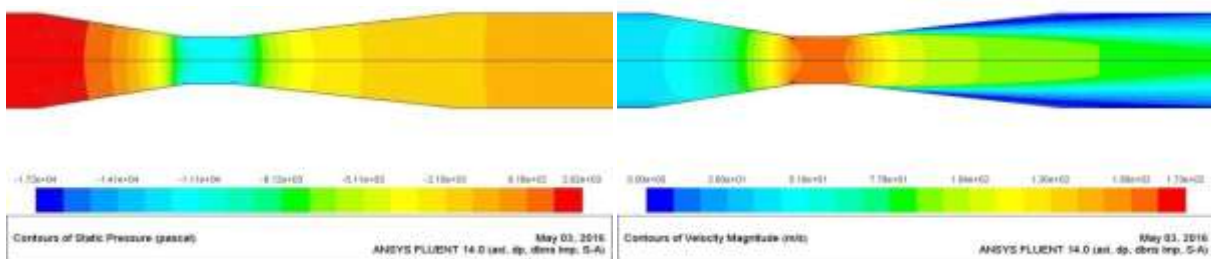


Figure 6(a) Pressure Contours

Figure 6(b) Velocity Contours

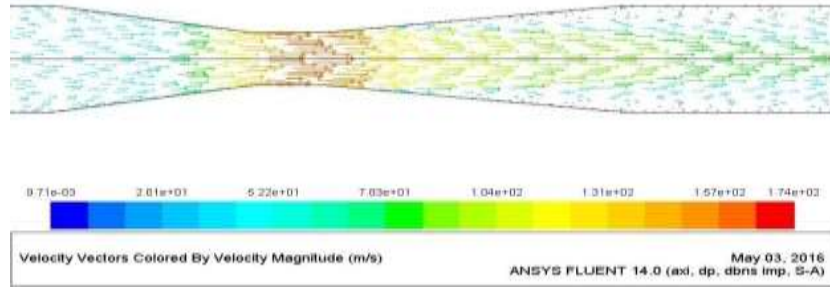


Figure 6(c) Velocity Vector

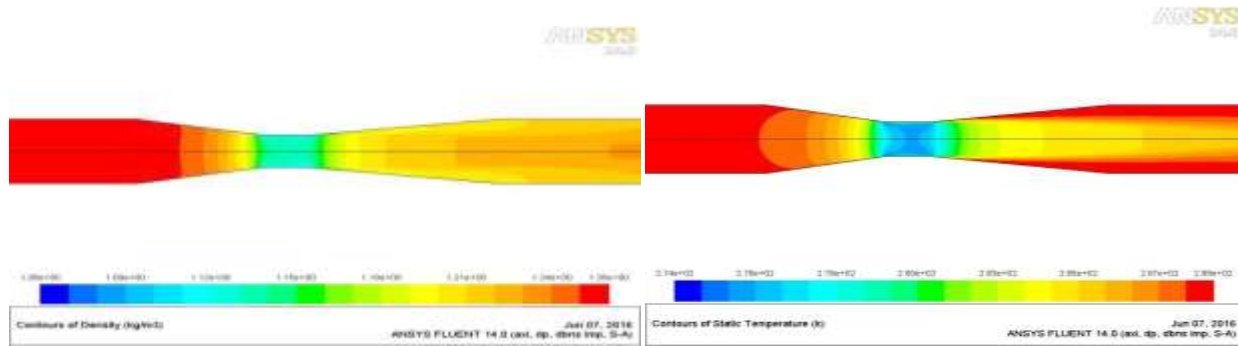


Figure 6(d) Density Contours

Figure 6(e) Temperature Contours

Figure 6 Contours and Vector Plots for Compressible Flow ($\beta=0.5, D=50\text{mm}, Re=6 \times 10^5$)

Permanent Pressure Loss Coefficient

The pressure loss caused by the Venturimeter can be determined by the pressure measurement made before and after installation of the Venturimeter in a pipe flows. The permanent pressure loss coefficient (C_{PL}) is the ratio of the pressure loss ($\Delta P^{11}-\Delta P^1$) to the differential pressure loss across the Venturimeter. The permanent pressure loss coefficient C_{PL} is given as

$$C_{PL} = \frac{\Delta p^{11}-\Delta p^1}{\Delta p_{\text{venturimeter}}} \quad (4)$$

Here,

Δp^1 is the pressure difference between the inlet and outlet of the pipe before the installation of the Venturimeter, the inlet of the pipe is at $-6D$ and outlet of the pipe is at $+20D$.

Δp^{11} is the pressure difference under the identical conditions after the installation of Venturimeter in the pipe.

$\Delta p_{\text{venturimeter}}$ is the pressure differential between the two pressure taps of the Venturimeter.

It is observed ΔP^{11} is always higher than ΔP^1 . For the purpose of calculating these parameters the upstream and downstream straight lengths of the tube are chosen as $6D$ and $20D$ respectively. It is observed from Table 4 that the permanent pressure loss coefficient (C_{PL}) decreases with increasing β ratio. This shows that pressure recovery after the venture becomes higher as the β ratio increases. It is also seen from the tabulated values that the computed values of C_{PL} are in close agreement with the values calculated on the basis of relation given in ISO 5167. The value of $(C_{PL})_{CFD}$ are in the range of 0.024 to 0.24. Its keeps on decreasing with increasing diameter ratio As per ISO 5167 the range in permanent pressure loss is generally between 5 % to 20% of the pressure differential of the meter CFD has been able to analyze exactly how this factor varies with diameter ratio.

Table 4 : Effect of Permanent Pressure Loss Coefficient for the Venturimeter for Incompressible Flow ($D=50\text{mm}$, $Re=6 \times 10^5$)

β	Δp^1 in (Pa)	Δp^{11} in (Pa)	Δp_{vent} in (Pa)	$(C_{\text{PL}})_{\text{CFD}}$
0.3	141625.56	2002.35	565609	0.2468
0.4	30406.25	2002.35	176032.2	0.1613
0.5	9089.50	2002.35	69498.77	0.1019
0.6	3741.02	2002.35	31162.08	0.055
0.7	2498.32	2002.35	14727.21	0.0336
0.75	2251.04	2002.35	10081.41	0.0246

The corresponding values calculated for the compressible flow are tabulated in the Table 5. It is observed that the value of C_{PL} in compressible flow with decreases with increases in diameter ratio.

Table 5 :Effect of Permanent Pressure Loss Coefficient for the Venturimeter for Compressible Flow ($D=50\text{mm}$, $Re=6 \times 10^5$)

β	Δp^1 in (Pa)	Δp^{11} in (Pa)	Δp_{vent} in (Pa)	$(C_{\text{PL}})_{\text{CFD}}$
0.3	2269.76	50.585	8578.78	0.2586
0.4	4803.32	296.257	29062.31	0.1550
0.5	2521.23	439.355	14561.91	0.1429
0.6	2141.22	854.90	13359.37	0.0962
0.7	2366.24	1628.37	12187.92	0.0605
0.75	2631.69	2121.41	10902.43	0.0469

B Effect of Wall Roughness in compressible flows

The wall rough nesses in the Venturimeter are also affecting the value of C_d of the Venturimeter. This affect can also analyze by varying roughness factor K/D in the range 0.1 to 0.02 in fact this six different value of K/D have been analyzed. Analyses have been made for both compressible and incompressible flows. The computed values are shown in the Table 6 and 7. ISO 5167-1 specifies the maximum roughness allowable for the different types of the Venturimeter.

As per ISO 5167-1 standard the allowable roughness height at the wall surface should be less than $0.0001D$. When a Venturimeter is installed in a pipe line due to continued corrosion/erosion, the surface becomes increasingly rough. In order to assess the effect of pipe roughness on the values of C_d and ϵ computations have been made with various rough nesses. Hence in this present work, while increasing the roughness height, how the compressibility effect changes is analyzed using the CFD analysis.

The simulation was carried out for the standard classical Venturimeter with the diameter of 50mm, β is 0.5 and Reynolds number is 6×10^5 . The results for the incompressible flow are tabulated in the Table 6. It is observed that if K/D is less than 2×10^{-5} then the value of C_d is not affected. Beyond this the value of C_d decreases. Thus for a roughness height of 0.1mm ($K/D=2 \times 10^{-3}$) the value of C_d is reduced by approximately 3%.

Table 6 : Effect of Wall Roughness on C_d from ISO 5167 for Incompressible Flow ($D=50\text{mm}$, $\beta=0.5$, $Re=6\times 10^5$)

Roughness height (mm)	K/D	C_d (ISO)	C_d (CFD)	Deviati on in %	$(C_d)_{\text{uncertain y}}$ in%
0	0	0.995	0.9850	1.01	1
0.001	$1*10^{-5}$	0.995	0.9850	1.01	1
0.005	0.0001	0.995	0.9820	1.32	1
0.01	0.0002	0.995	0.9782	1.71	1
0.1	0.002	0.995	0.9635	3.26	1
1	0.02	0.995	0.9594	3.71	1

Similar computations have been repeated for compressible flow for the same Venturimeter under identical conditions. The Comparison between the computed and codal values of C_d and ϵ for Venturimeter is listed in the Table 7 for compressible flow. It is observed from the tabulated values the values of C_d and ϵ for the compressible flows is not effected by pipe roughness significantly however a close look at the values of $(C_d)_{\text{com}}$ reveals that the values of both $(C_d)_{\text{com}}$ and ϵ increase with increases in roughness. However the increase is of the order of 1% only. It is also observed that the effect of roughness is much more pronounced on the value of $(C_d)_{\text{incom}}$

Table 7 :Comparison between the Computed and Standard Values of C_d and ϵ for Compressible Flow ($D=50\text{mm}$)

Roughness height (mm)	K/D	$\Delta p/p_1$	$(C_d)_{\text{inc}}$	$(C_d)_{\text{com}}$	ϵ (CFD)	ϵ (ISO)
0	0	0.096	0.985	0.925	0.939	0.942
0.001	0.00002	0.096	0.985	0.925	0.939	0.942
0.005	0.0001	0.096	0.982	0.925	0.942	0.942
0.01	0.0002	0.096	0.978	0.924	0.945	0.942
0.1	0.002	0.099	0.963	0.911	0.946	0.940
1	0.02	0.099	0.959	0.912	0.951	0.940

C Effect of Turbulence Intensity on Compressible Effect

The turbulence intensity plays a very important role in the flow characteristics in the pipe. Hence in this present study, computations are made for various values of the turbulence intensity in the incoming flow in order to analyze the effect of this parameter on the compressibility effects in the Venturimeter. The simulation was carried out for the standard classical Venturimeter with the diameter of 50mm and β is 0.5 with order of Reynolds number is 6×10^5 .

It is observed from tabulated values in Table 8 that the level of turbulence intensity in the incoming flow has no significance influence on the value C_d of the Venturimeter. The range of turbulence intensity covered is 0.1 to 10%.

Table 8 : Effect of Turbulence Intensity on Discharge Coefficient from ISO 5167-1 for Incompressible Flow ($D=50\text{mm}$, $\beta=0.5$, $Re=6 \times 10^5$)

Turbulence intensity in %	$C_d(\text{ISO})$	$C_d(\text{CFD})$	Deviation in %
0.1	0.995	0.9846	1.05
0.2	0.995	0.9845	1.06
1	0.995	0.9843	1.08
5	0.995	0.9839	1.12
10	0.995	0.9839	1.12

The Comparison between the computed and codal values of C_d and ϵ for Venturimeter for different turbulent intensity is listed in the Table 9 for compressible flow. In this case also it is observed that the turbulence intensity has no significant effect on the value of C_d and ϵ for the flow of compressible fluids.

Table 9 : Comparison between the Computed and Standard Values of C_d and ϵ for Compressible Flow ($D=50\text{mm}$)

Turbulence intensity in %	$\Delta p/p_1$	$(C_d)\text{incom}$	$(C_d)\text{com}$	ϵ (CFD)	ϵ (ISO)
0.1	0.870	0.9846	0.8897	0.9036	0.9130
0.2	0.732	0.9845	0.8893	0.9033	0.9141
1	0.646	0.9843	0.8833	0.8973	0.9141
5	0.422	0.9839	0.8828	0.8972	0.9142
10	0.335	0.9839	0.8929	0.9075	0.9149

D Effect of Variation in the Convergent and Divergent Angles

Classical Venturimeter are complex to manufacture and also the cost involved in the manufacture is somewhat higher. Hence many a times to make the flow meter more compact and economical the convergent and divergent angles are increased beyond the specified values of ISO 5167 standard (as in the case of Venturinozzle). Hence computation have been made for different values of convergent and divergent angles while keeping the other parameters constant and analysis has been made for both incompressible and compressible flows. The simulation was carried out for the standard classical Venturimeter with the diameter of 50mm, β is 0.5 and Reynolds number is 6×10^5 .

ISO 5167 specifies the semi convergent angle (2θ) is less than $21 \pm 1^\circ$ and divergent angle (2ϕ) is 7° to 15° . In many cases larger angles may be used due to space and cost constraints in certain applications. Hence computations have been made with various convergent and divergent angles and results are summarized in the Table 10.

It is observed that increasing convergent angle beyond in the specification of ISO 5167 while keeping divergent angle within the limits, the values of C_d in incompressible fluid is not affected very significantly. Further keeping semi convergent angle 20° and increasing the semi divergent angle up to 15° the results show a marginal decrease in C_d .

Table 10 : Effect of Convergent and Divergent Angle on Discharge Coefficient from ISO 5167-1 for Incompressible Flow

θ in deg	Φ in deg	$C_d(\text{CFD})$	$C_d(\text{ISO})$	Deviation in %	$(C_d)_{\text{uncertainty}}$ in%
10	7	0.995	0.9885	0.65	1
12.5	7	0.995	0.9878	0.72	1
15	7	0.995	0.9867	0.84	1
20	10	0.995	0.9861	0.90	1
20	12.5	0.995	0.9850	1.01	1
21	15	0.995	0.9822	1.30	1

The Comparison between the computed and codal values of C_d and ϵ for Venturimeter is listed in the Table 11 for compressible flow. The conclusion drawn from the incompressible flow is also valid for compressible flow the effect of variation in θ and ϕ on the values of C_d and ϵ is only minor.

Table 11 : Comparison between the Computed and standard Values of C_d and ϵ for compressible flow ($D=50\text{mm}$, $\beta=0.5$)

θ in deg	ϕ in deg	$\Delta p/p_1$	$(C_d)_{\text{incom}}$	$(C_d)_{\text{com}}$	ϵ (CFD)	ϵ (ISO)
10	7	0.0965	0.9885	0.9258	0.936	0.942
12.5	7	0.0967	0.9878	0.9197	0.931	0.941
15	7	0.0968	0.9867	0.9248	0.937	0.942
20	10	0.0970	0.9861	0.9236	0.936	0.942
20	12.5	0.0971	0.9850	0.9235	0.937	0.942
21	15	0.0979	0.9822	0.9234	0.940	0.941

Permanent Pressure Loss Coefficient

The value of C_{PL} has defined in Eqn.6 have be calculated for both compressible and incompressible flows for various values of θ and ϕ . The results are tabulated in Table 12. It is observed from the tabulated values in Table 12 that for incompressible flow, the permanent pressure loss coefficient (C_{PL}) is dependent on convergent and divergent angles. As long as these angles are within the specified limits of ISO 5167 the computed values of C_{PL} are in agreement with the values given in code.

It is observed the changes in semi convergent angle from 10° to 15° keeping the semi divergent angle as 7° doesn't affect the value of C_{PL} significantly. However the increase in the divergent angle from 7° to 15° increases the pressure loss coefficient from 0.16 to 0.41. This shows that the permanent pressure loss in the case of Venturimeter is strongly dependent on the divergent angle. As the divergent angle increases beyond 7° the losses due to separation increases and hence this results in additional pressure loss.

Table 12 : Effect of Permanent Pressure Loss Coefficient for the Venturimeter for Incompressible Flow ($D=50\text{mm}$, $\beta=0.5$)

θ in deg	ϕ in deg	Δp^{11} in (Pa)	Δp^1 in (Pa)	$\Delta p_{\text{venturi}}$ in (Pa)	$(C_{PL})_{\text{CFD}}$
10	7	1894.8	344.67	9854.39	0.1573
12.5	7	1957.7	344.67	9985.57	0.1615
15	7	1960.6	344.67	9989.31	0.1617
20	10	2731.1	344.67	9977.49	0.2391
20	12.5	3059.3	344.67	9995.67	0.2715
21	15	4452.2	344.67	10129.71	0.4054

The corresponding values calculated for the compressible flows are tabulated in the Table 13. It is observed from the tabulated values the deviation of C_{PL} for compressible flow is similar to that observed for incompressible flow. However a comparison between the values of C_{PL} in Table 12 and 13 shows that the magnitude of C_{PL} are lower in compressible flow. Once again the convergent angle has only a minor affect on the C_{PL} provided the divergent angle is kept at the standard value. Increasing the θ value from 10° to 15° the value of C_{PL} changes from 0.07 to 0.1. However as the divergent angle increases from 7° to 15° the value of C_{PL} increases from 0.1 to 0.234 the reason for this increase has already been explained in the discussion of incompressible flow results.

Table 13 : Effect of Permanent Pressure Loss Coefficient for the Venturimeter for Compressible Flow ($D=50\text{mm}$, $\beta=0.5$)

θ in deg	ϕ in deg	Δp^1 in (Pa)	Δp^{11} in (Pa)	$\Delta p_{\text{venturi}}$ in (Pa)	$(C_{PL})_{\text{CFD}}$
10	7	6710.19	2002.3	69039.6	0.0681
12.5	7	7344.61	2002.3	69200.88	0.0771
15	7	8748.09	2002.3	69438.26	0.0971
20	10	9629.35	2002.3	69279.84	0.1100
20	12.5	16629.5	2002.3	119676.8	0.1222
21	15	18251.9	2002.3	69441.2	0.2340

CONCLUSION

CFD modeling and simulation was performed to demonstrate the capability of the CFD methodology to analyze the compressibility effect in the classical Venturimeter. The results obtained from CFD were used to study the detailed information on the Venturimeter flow characteristics that could not be easily measured during experimental tests. The validated CFD methodology has been used to analyze the flow through the classical Venturimeter for both incompressible and compressible flows. The computed values of the C_d , ε and C_{PL} are in good agreement with the values given in ISO 5167. It is also been demonstrated that the validated CFD methodology can be used to predict the performance characteristics of the Venturimeter even outside the limits specified in ISO 5167.

The validated CFD methodology has been used to analyze the effect of several parameters like convergent and divergent angle, wall roughness and turbulence intensity. It is observed that increase in the convergent-divergent angles beyond the standard values has no significant effect on the values of C_d and ε . However increase in the divergent angle results in significant increase in the value of C_{PL} . Increase in the value of relative wall roughness factor (K/D) beyond 0.00001, decreases the value of C_d for incompressible flow. However the values of ε and C_d for

compressible flow are not very much affected. Increase in the turbulent intensity of the incoming flow from 0.1 to 10% doesn't alter the values of performance parameters of the Venturimeter significantly.

REFERENCES

1. Gordon Stobie, Conoco Phillips, Robert Hart and Steve Svedeman, Southwest Research Institute. "Erosion in a Venturi Meter with Laminar and Turbulent Flow and Low Reynolds Number Discharge Coefficient Measurements". International Journal of Mechanical, Aerospace, Industrial, Mechatronic and Manufacturing Engineering Volume:8, No.3,2014.
2. Diego A.Arias and Timothy A.Shedd, "CFD Analysis of Compressible Flow across A Complex Geometry Venture" *J. Fluids Eng* 129(9), 1193-1202 (Apr 10, 2007) (10 Pages)
3. Arun R, Yogesh Kumar K J, V Seshadri, "Prediction of Discharge Co Efficient of Venturimeter at Low Reynolds Numbers By Analytical and CFD Method", Internal National Journal of Engineering and Technology and Technical Research, ISSN: 2321-0869, Volume-3, Issue-5, and May 2015.
4. Kenneth.C.Cornellus, Kartik Srinivas, "Isentropic Compressible Flow for Non Ideal Gas Model for Venture", International Journal, IET Communications, Vol. 2, Issue 2.
5. Nikhil Tamhankar, Amar Pandhare, Ashwinkumar Joglekar, Vaibhav Bansode (2014) "Experimental and CFD analysis of flow through Venturimeter to determine the coefficient of discharge", International Journal of Latest Trends in Engineering and Technology
6. Arun R (2014), "Prediction of Characteristics of Venturimeter at Non Standard Conditions Using CFD", M Tech Thesis, MIT Mysore, VTU 2015.
7. Indian standard ISO-5167-1, Measurement of fluid flow by means of pressure differential devices (1991).